Ecological Indicators 168 (2024) 112804

Contents lists available at ScienceDirect

Ecological Indicators

journal homepage: www.elsevier.com/locate/ecolind

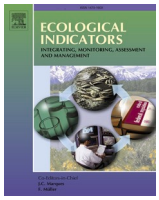

Assessment and prediction of habitat risk on the Qinghai-Xizang plateau under multiple scenarios

Farui Jiang [a,b], Shaofen Xu [c], Chonghao Liu [a,d,*], Jianan Zhao [e], Baode Jiang [b], Fengyan Fan [a,d]

[a] Institute of Mineral Resources, Chinese Academy of Geological Sciences, Beijing 100037, China
[b] China University of Geosciences (Wuhan), Wuhan 730078, China
[c] Department of Land Surveying and Geo-Informatics, The Hong Kong Polytechnic University, Hung Hom, Hong Kong
[d] Research Center for Strategy of Global Mineral Resources, Chinese Academy of Geological Sciences, Beijing 100037, China
[e] Guangdong Mineral Resources Exploration Institute, Guangdong Geological Bureau, Guangdong, Guangzhou 510062, China

ARTICLE INFO

Keywords:
Qinghai-Xizang plateau
Habitat risk assessment
Human footprint index
Grazing intensity
Multilayer perceptron
PLUS Model

ABSTRACT

The Qinghai-Xizang Plateau (QXP), the highest plateau in the world, boasts a diverse array of ecological landscapes shaped by extreme climatic conditions; however, it is currently facing significant ecological challenges. In recent years, an increase in human activities, particularly the expansion of the human footprint and grazing intensity, has significantly exacerbated the pressures on habitat risk in the region. In this context, the future habitat risk trend under different scenarios on the QXP require further investigation. To address this gap, a comprehensive multi-scenario habitat risk prediction methodology was developed to fill this gap by integrating the InVEST model, the patch-generating land use simulation model, and the multilayer perceptron model, which combined land use and land cover data with human footprint index and grazing intensity data for a thorough assessment and prediction of habitat risk. Specifically, spatiotemporal changes in habitat risk on the QXP from 2000 to 2020 were analyzed, future indicators were projected, and spatiotemporal variations in habitat risk were evaluated under multiple scenarios. The findings indicate that high-risk areas experienced a significant increase of 39% in 2005; however, this was subsequently mitigated by protective measures. In the Ecological Protection scenario, high habitat risk was reduced by over 74%, while the Urban Development scenario saw an increase of 81% in high habitat risk. The alterations in habitat risks observed between 2005 and 2010 indicate that ecological conservation efforts on the Qinghai-Xizang Plateau have been effective. Among the various development pathways, the Ecological Protection scenario appears to be the most viable for the QXP. Nonetheless, the central and eastern regions of the QXP may continue to face an upward trend in habitat risk.

1. Introduction

The Qinghai-Xizang Plateau (QXP, historically referred to as the Qinghai-Tibet Plateau) serves as a crucial ecological barrier for China, with its vast glaciers and snow reserves playing a pivotal role in regulating Asian climate (Hua et al., 2022). The high-altitude environment and unique climate system significantly influence the Asian monsoon system and regional hydrological cycles while serving as a critical global biodiversity hotspot with numerous endemic species (Liu, 2021; Sun et al., 2023a, 2023b). However, despite its critical role in global climate regulation, the plateau's ecosystem displays pronounced vulnerability. Previous studies indicate a significant decline in meadow area in the northeastern region of the plateau (Wang et al., 2008), and the urban expansion has led to the deterioration of wetlands, exacerbating the ecological challenges faced by this already fragile region (Nie et al., 2022). Pressured by both global climate change and human activities, it faces severe environmental challenges, including accelerated glacier retreat, permafrost degradation, grassland deterioration, intensified soil erosion, biodiversity loss, depletion of rare wildlife resources, and frequent natural disasters (Liu and Chen, 2023; Liao et al., 2022; Wang et al., 2024; Drucker et al., 2011; Yang et al., 2024; Zhou et al., 2024). These issues significantly undermine the plateau's function as a regional ecological security barrier (Xue et al., 2023). Over the past decades, the Chinese government has implemented a range of ecological protection policies on the QXP, including ecological benefit compensation, ecological security barrier protection, and transfer payments for critical

* Corresponding author at: No. 26, Baiwanzhuang Street, Xicheng District, Beijing, China.
E-mail address: hawking.2@163.com (C. Liu).

https://doi.org/10.1016/j.ecolind.2024.112804
Received 20 July 2024; Received in revised form 17 October 2024; Accepted 31 October 2024
Available online 4 November 2024

ecological function areas (Wang et al., 2021). Additionally, the government has launched the Sanjiangyuan Nature Reserve ecological protection project ecological protection project and established ecological red lines (Zhao et al., 2023; Nie et al., 2023; Gu et al., 2023). The intensity of ecological and environmental policy protection has been progressively strengthened.

For the evaluation of ecosystems, habitat serves as a crucial indicator for evaluating the spatial extent of an organism's survival within an ecological environment. Habitat Risk Assessment (HRA), which examines the cumulative impacts of anthropogenic stressors on habitats, is essential for preserving ecologically sensitive areas and for species conservation (Arkema et al., 2015). It provides a necessary framework for understanding and mitigating risks to ecosystems and their inhabitants, ensuring the sustainability of biodiversity (Zhang et al., 2022; Zhu et al., 2022). Previous studies have proven that HRA effectively uses land use data for habitat risk assessment and has been successfully applied in numerous locations worldwide (Yu et al., 2024a, 2024b; Arkema et al., 2014; Cabral et al., 2015; Chung et al., 2015; Duggan et al., 2015; Wyatt et al., 2017). However, previous habitat risk assessment studies often overlook the ecological vulnerability of the QXP, which stems from its unique natural environment and increasing pressures from human activities, particularly the human footprint and grazing intensity (Fetzel et al., 2017; Zhang et al., 2018). The formulation of effective environmental protection policies should assess historical habitat risks and consider changes in future habitat risks under different scenarios. Previous studies on habitat tended to focus more on land use change and to combine human impacts into a single index, that is, human activity (Bai et al., 2019; Hack et al., 2020; Liu and Chen, 2023). However, given the QXP's relatively low population density and the prevalence of grazing farming, it is essential to discuss the human footprint and grazing intensity separately. This approach allows for a more nuanced understanding of how these distinct human activities impact the ecosystem and habitat risks. By disentangling the effects of human footprint and grazing intensity, policymakers and conservationists can develop more targeted and effective strategies to mitigate ecological risks and promote sustainable land use practices on the plateau. Therefore, it is necessary to incorporate new dynamic indicators, such as the human footprint index (HFI) and grazing intensity (GI), into the habitat risk assessment framework while integrating multiple models to construct a multi-scenario habitat risk prediction framework.

In addition to analyzing historical habitat risk changes based on past and current data, forecasting future condition is also critical for ecological management and conservation regarding future habitat risks under different scenarios. To predict changes in land use patterns, the Patch-generating Land Use Simulation (PLUS) model has proven particularly effective in forecasting complex environmental changes (Liang et al., 2021). The PLUS model simulates LULC changes by dynamically capturing the evolution of multiple land use patches. It integrates the Land Expansion Analysis Strategy (LEAS), and a Cellular Automaton model based on multi-type random patch seeds (CARS), offering a more precise simulation of land use change processes and trends (Wang et al., 2023a, 2023b). This model is precious for understanding the driving forces behind land expansion and predicting landscape dynamics (Guo et al., 2023a, 2023b; Liu et al., 2023b).

However, the PLUS model is more inclined toward handling discrete categorical data. Machine learning has introduced more flexible and adaptive methods for predicting complex ecological dynamics for continuous intensity indicators. The Multilayer Perceptron (MLP) neural network is renowned for its ability to approximate nonlinear functions and is particularly effective at capturing the dynamic relationships between various factors within ecosystems. By automatically learning data patterns, MLP eliminates the need for manual feature engineering. It excels in handling high-dimensional datasets, making it an ideal tool for predicting changes in vital ecological indicators (Xu et al., 2022; Kumar et al., 2023; Moayedi et al., 2023).

Accordingly, the aim of this study is to assess and predict habitat risk on the QXP, as well as to clarify whether more favorable policy management can mitigate habitat risks, particularly in high-risk areas, when further considering the increasing pressure of human activities. Additionally, under different future development scenarios, we investigate the extent to which varying levels of policy implementation, land use changes, and human activities will result in different habitat risk outcomes, and which future development scenario is most likely. To address these questions, we have established three specific research objectives: (1) incorporating new indicators, such as grazing intensity and human footprint index, to develop a habitat risk assessment tailored to the unique ecological environment of the plateau. (2) Integrating multiple models to construct a comprehensive, multi-scenario habitat risk prediction framework that addresses various development needs specific to the plateau. (3) Assessing the impact and effectiveness of policy through the changes in habitat risk areas under multiple past and future scenarios while comparing existing policies to predict the most likely development path in the future.

2. Study area and data

2.1. Study area

The QXP, located in southeast China, is characterized by an average elevation surpassing 4000 m and a total area of approximately 2.5 million km^2 (Sun et al., 2023a, 2023b) (Fig. 1). This region features a complex terrain, composed of vast plateaus, steep mountains, and deep valleys, forming a unique highland mountainous geomorphological system. Climatically, the QXP is characterized by cold and dry conditions, with significant annual temperature variation and minimal diurnal temperature variation. Precipitation levels vary significantly across different areas (Drucker et al., 2011; Yang et al., 2024). The vegetation cover on the QXP is closely related to its topography and climate, ranging from arid and barren alpine deserts to lush alpine meadows and forests, showcasing diverse landscapes and ecological system structures (Zhou et al., 2024).

Despite the relatively low level of urbanization on the QXP, there has been growing concern over the rapid increase in urban population and the rapid expansion of construction land in recent years (Wang et al., 2020). The construction and operation of the Qinghai-Xizang Railway and the Sichuan-Xizang Railway may pose potential risks to the local ecological environment (Cui et al., 2022). At the same time, livestock farming, which is a significant production activity on the QXP, has exacerbated grassland degradation over the past 20 years due to climate change and intensified grazing activities (Chen et al., 2022), further leading to the loss of biodiversity (Liu et al., 2023a).

2.2. Data collection

This study utilizes the 30 m resolution land use data for five periods (2000, 2005, 2010, 2015, and 2020) published by the Resources and Environmental Sciences, Chinese Academy of Sciences (RESDC) (https://www.resdc.cn). The data categorize land use into six primary types: plowland forestland, meadow, water bodies, town land, and unused land, where town land refers to villages and small settlements and includes construction land.

Seven factors were selected to calculate the intensity of HFI: GDP (Chen et al., 2022; https://www.resdc.cn), PopD (https://landscan.ornl.gov/), NL (Chen et al., 2022), roads (https://www.openstreetmap.org), railways (https://www.openstreetmap.org), plowland, and town area. These data spanned from 2000 to 2020. GI data for the QXP were also employed (Liu, 2021). The GI data was available annually from 2000 to 2019. Considering the absence of GI data for 2020, we used the 2019 data as a substitute.

To calculate the development potential of different land types, 12 driving factors were used, including GI, precipitation (Peng, 2020),

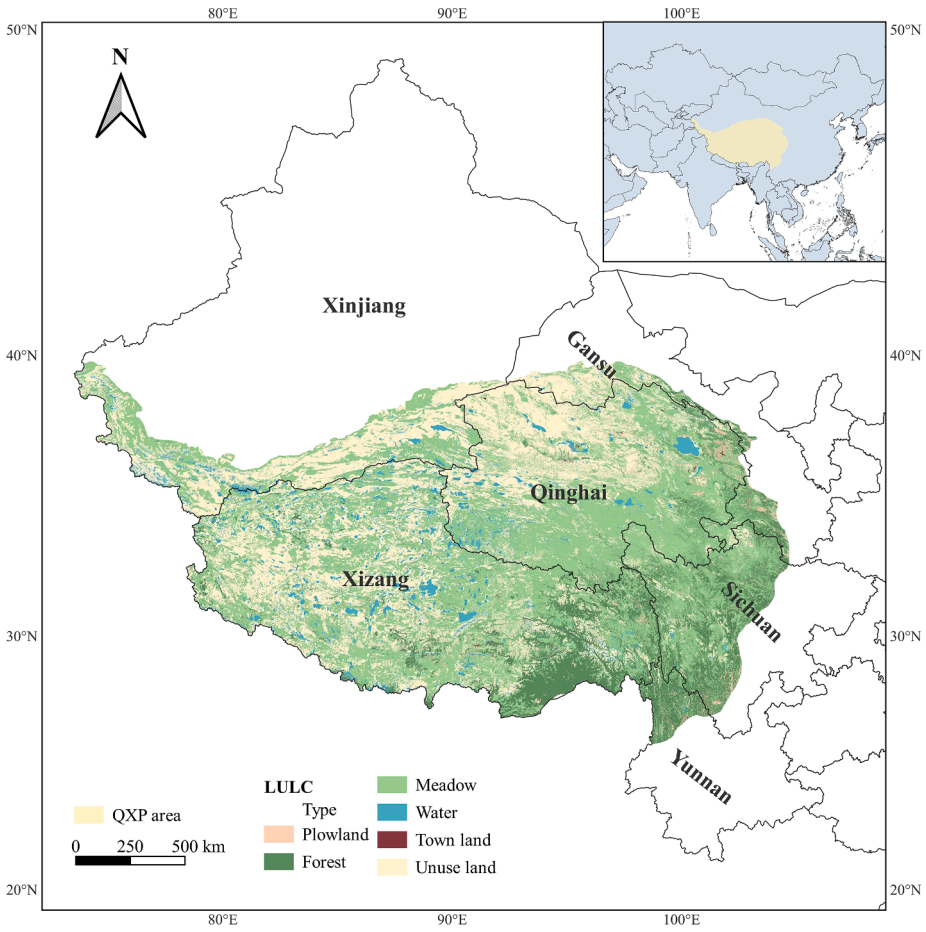

Fig. 1. Geographic location, land use types and vegetation zonation of the Qinghai-Xizang Plateau. LULC data derived from Chinese Academy of Sciences, vegetation zoning data derived from Vegetation Atlas of China.

temperature (Peng, 2023), DEM (https://www.gscloud.cn), slope, HFI, distance to primary roads, distance to secondary roads, distance to tertiary roads, distance to trunk roads, distance to railways, and distance to water bodies.

Data from national nature reserves (https://www.gisrs.cn) were used to constrain HFI and GI further. All data of different resolutions were converted uniformly to 300 m resolution and projected as EPSG: 3857-WGS 84/Pseudo-Mercator. Table 1 provides detailed information on the data sources.

3. Methodology

To evaluate and forecast habitat risk in the QXP, this study comprehensively assesses habitat risks under multiple scenarios by integrating LULC data with HFI and GI data.risks The HRA module within the InVEST model quantifies spatiotemporal shifts in habitat risk from 2000 to 2020. The PLUS model is employed to extract land use expansion, using 12 driving factors to calculate the development potential of different land use types. Three distinct scenarios are formulated: business-as-usual (BAU), ecological protection (EP), and urban development (UD). Land use changes in the QXP from 2025 to 2035 are simulated under these scenarios. The MLP model is trained using annual data on PopD, NL, and GDP from 2000 to 2020 and GI from 2000 to 2019 to forecast PopD, NL, GDP, and GI under each scenario. The spatiotemporal changes in habitat risks and risk are quantitatively assessed on the QXP from 2025 to 2035 based on the HRA module within the InVEST model (Fig. 2).

3.1. Habitat risk assessment

The Habitat risk assessment (HRA) based on the InVEST model is a quantitative method used to evaluate the cumulative risk to habitats or species from multiple stressors (Arkema et al., 2015). The model includes two dimensions of information, exposure (E) and consequence (C), used to calculate the risk or impact on ecosystem components. Here, E represents the degree of exposure of a specific habitat to a particular human activity, while C represents the response of that habitat to a specific level of exposure, including its resistance to and recovery from the exposure stressors. The values of E and C can be calculated using the following formulas (Eqs. (1) & (2)):

$$E = \frac{\sum_{i=1}^{N} \frac{e^k}{d_k \omega_k}}{\sum_{i=1}^{N} \frac{1}{d_k \omega_k}} \tag{1}$$

$$C = \frac{\sum_{i=1}^{N} \frac{c^k}{d_k \omega_k}}{\sum_{i=1}^{N} \frac{1}{d_k \omega_k}} \tag{2}$$

where d_k represents the data quality score under an indicator k, which can be assigned different values based on the data quality. ω_k denotes the importance score of the data under the indicator k, representing the importance weight of the indicator k. N is the number of indicators used to evaluate each habitat. Based on the above calculations for E and C, the risk value R_{ij} for each stressor j on a habitat i can be further determined. The risk value R_{ij} can be obtained using the Euclidean risk calculation formula (Eq. (3)) or the multiplicative risk calculation formula (Eq. (4)).

Table 1
Data types and sources.

Data type	Data sources	Format	Scale
LULC	Resources and Environmental Sciences, Chinese Academy of Sciences (RESDC) (https://www.resdc.cn)	raster	30 * 30 m
Vegetation zoning	Editorial Board of the Vegetation Atlas of China, Chinese Academy of Sciences. Vegetation Atlas of China. Beijing: Science Press, 2001.	vector	/
Population density	LandScan Global, LandScan High-Definition (HD), and LandScan USA	raster	1000 * 1000 m
GDP	Chen et al., 2022; Resources and Environmental Sciences, Chinese Academy of Sciences (https://www.resdc.cn)	raster	1000 * 1000 m
Night lighting	Chen et al. (2020a) and Chen et al. (2020b)	raster	1000 * 1000 m
GI	Liu, 2021	raster	250 * 250 m
Road	OpenStreetMap contributors. (2000–2020). Road network data. Retrieved from https://www.openstreetmap.org	vector	/
River	Adc, W. (2019). The Third Pole 1:1,000,000 river dataset (2014). National Tibetan Plateau / Third Pole Environment Data Center	vector	1:1,000,000
DEM	Geospatial Data Cloud site, Computer Network Information Center, Chinese Academy of Sciences. (https://www.gscloud.cn)	raster	30 * 30 m
Slope	Geospatial Data Cloud site, Computer Network Information Center, Chinese Academy of Sciences. (https://www.gscloud.cn)	raster	30 * 30 m
Average annual temperature	Peng, 2020	raster	1000 * 1000 m
Average annual precipitation	Peng, 2023	raster	1000 * 1000 m
Nature reserve	Geographic remote sensing ecological network platform (https://www.gisrs.cn)	vector	/

$$R_{ij} = \sqrt{(E-1)^2 + (C-1)^2} \tag{3}$$

$$R_{ij} = EC \tag{4}$$

In assessing model indicators, this study incorporates a comprehensive survey of the actual conditions in the study area and relevant environmental protection policies. Referring to the InVEST User Guide, the study considers habitats' natural recovery time and calculates ***E*** based on temporal overlap, management effectiveness, and intensity level. ***C*** is calculated based on area ratio change, disturbance frequency, and structure change level (Supplementary Tables 1 and 2).

From 2000 to 2005, policy management for meadows was relatively weak, while management for forests and water bodies was somewhat stricter. Between 2010 and 2015, management efficiency for meadows, forests, and water bodies was further enhanced. By 2020, management efficiency peaked, reflecting significant advancements in ecological protection efforts.

3.2. Human footprint index (HFI) assessment

This study selected seven factors to calculate the human footprint index: GDP, PopD, NL, roads, railways, plowland, and town area. The raw raster data were pre-processed, and scores were calculated by category as well as intensity (Table 4) to obtain the human footprint index dataset, which was calculated as follows:

$$HFI(i,t) = \sum_{i=1}^{7} \omega_i \alpha_i = \frac{PopD}{3} + \frac{NL}{3} + \frac{GDP}{3} + PL + TL + R + RW \tag{5}$$

where *HFI* is human footprint index, *PopD* is population density; *NL* is nighttime light intensity; *GDP* is gross domestic product per capita; *PL* is Plowland; *TL* is town land; *R* is road; and *Rw* is railway. In this calculation, α represents one of the seven indicators, and ω denotes the corresponding weight. The HFI is calculated by summing the normalized values of the seven variables according to Eq. (5). Given the potential correlations between PopD, GDP, and NL, we assigned lower weights to these indicators based on prior research (Liu et al., 2023b). The indirect pressures of human activities on road infrastructure and land use areas were also assessed to evaluate their further impacts (Table 2).

3.3. Simulation of land use expansion in multiple contexts based on PLUS modeling

The PLUS model consists of three components: Land Expansion Extraction, LEAS, and CARS. First, areas of land expansion are identified by comparing two historical land use maps. The LEAS module uses the land expansion map and the driving factors of LULC to assess the development potential of each land type. Finally, the CARS component utilizes the initial land use and development potential obtained from LEAS to simulate future land use patterns. This model can accurately simulate the processes and trends of land use changes, providing essential tools and methods for geographic research.

In this study, based on the actual conditions of the QXP and references from related research by other scholars (Guo et al., 2023a, 2023b; Lin and Fu, 2023; Wang et al., 2023a, 2023b), 12 driving factors were identified. The development probability of each land use type and the contribution of each driving factor to the expansion of various land use types during the period were calculated. The specific calculation method is as follows (Eq. (6)) (Lin and Fu, 2023):

$$P_i k_d(x) = \sum n = 1MI = [hn(x) = d]M \tag{6}$$

where, $P_i k_d(x)$ represents the probability of land use type k appearing in unit i, where d is either 1 or 0, and x is a vector composed of multiple driving factors. The function I is the indicator function of the decision tree ensemble, $hn(x)$ indicates the predicted type of the decision tree, and M is the total number of decision trees.

3.4. Future scenario settings

This study constructs three land use change scenarios to better promote the harmonized advancement of urban development, farmland conservation, and ecological environment preservation within the QXP. These scenarios are formulated by integrating findings from pertinent scholarly work and considering the region's environmental development and conservation policies (Supplementary I).

(1) Business-as-usual (BAU): This scenario is predicated on historical observational data and established developmental trajectories. It projects the progression and transformation of land use categories without novel conservation initiatives or land management paradigms. It refrains from imposing supplementary constraints on the transmutation between disparate land use types, thereby serving as a foundational benchmark against which alternative scenarios are assessed, particularly those about ecological safeguarding and urban advancement.
(2) Ecological Protection (EP): Based on the national legislative framework for environmental conservation and ecological restoration on the QXP, this scenario imposes more rigorous ecological preservation mandates. It limits transforming meadows, forest land, and water bodies to farmland or construction land. The scenario also integrates data about the QXP's

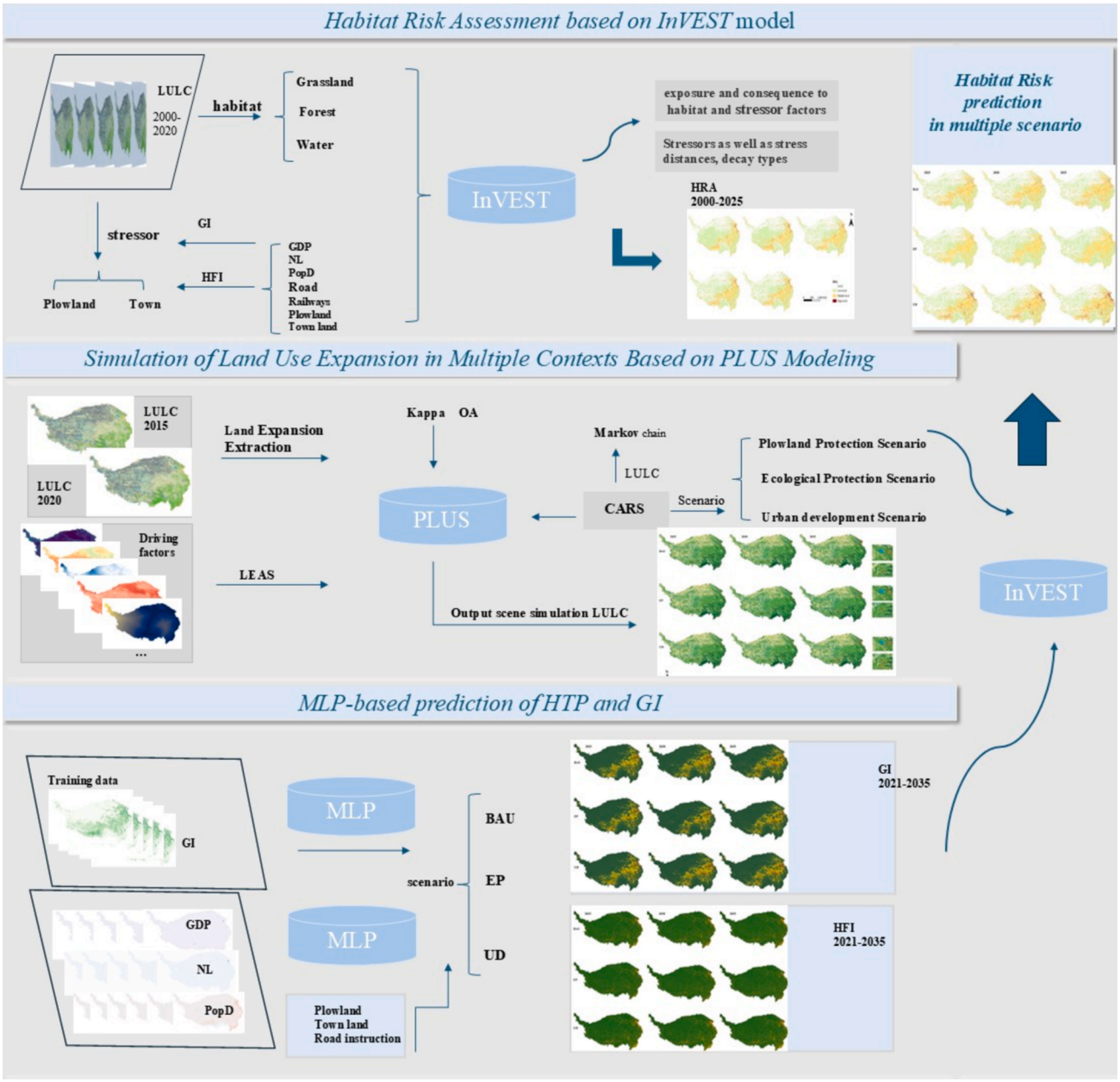

Fig. 2. Research Technology Roadmap. The process consists of three main steps: Calculating past changes in habitat risk, predicting changes in LULC, GI, and HFI under multiple scenarios, and assessing habitat risk variations under these scenarios.

nature reserves, enforcing land-use conversion restrictions within these protected zones to ensure their integrity and conservation. Furthermore, it strategically expands the aggregate expanse of meadow, forest, and water body areas by incrementally increasing their coverage, which in turn elevates the likelihood of the transmutation of other land use types into these ecological categories, reinforcing the resilience of the QXP's ecological systems.

(3) Urban Development (UD): Focused on stimulating economic expansion and the progression of urbanization, the UD scenario adopts a more lenient approach to the stringent preservation of meadow, forest land, and water bodies. This approach facilitates an enlargement of the built-up land area, accommodating the spatial demands of urban sprawl. Concurrently, it raises the likelihood of reclassifying other land use types to construction land, thereby supporting the infrastructural and demographic growth associated with urban centers, aligning with the objectives of metropolitan expansion and economic vitality.

3.5. MLP-based prediction of HFI and GI

The MLP is designed to leverage multiple time steps of input data for predictive modeling. Specifically, the model leverages three consecutive years of historical data to predict future values. Initially, the connections between neurons are initialized with random weights. The input layer receives the preprocessed data, including adjustments for grassland boundaries and conservation area weights, and sends it to the hidden layers, enables the MLP to accurately predict GDP, NL, PopD and GI on the QXP using historical data under multi-Scenario simulations.

To efficiently manage extensive image data, the data is segmented into overlapping chunks that are processed independently. This approach reduces memory usage and ensures smooth integration of predictions. The training data is standardized using techniques like the

Table 2
Data description, source, impact range and references for the human footprint index (HFI).

Type	Score	Indirect impact range	Descriptions	References
PopD	[0,9]	/	For all areas with a population density exceeding 1000 people per km^2, we assigned a maximum score of 9. The remaining areas were scored on a 0–9 scale at equal intervals.	Venter et al. (2016) and Williams et al. (2020)
NL	[0,9]	/	For all areas with nighttime light intensity greater than 10 per km^2, we assigned a maximum score of 9. The remaining areas were scored on a 0–9 scale at equal intervals.	
GDP	[0,9]	/	For all areas with a GDP more significant than 10 per km^2, we assigned a maximum score of 9. At equal intervals, the remaining areas were scored on a 0–9 scale.	
Plowland	0,4,8	800 m	Areas classified as "Plowland" are assigned a maximum score of 8. Regions within an 800-m indirect impact range of these areas receive 4 points, while all other areas are assigned 0 points.	Liu et al. (2023b)
Town land	0,5,10	1000 m	Areas classified as "town land" are assigned a maximum score of 10. Regions within a one-kilometer indirect impact range of these areas receive 5 points, while all other areas are assigned 0 points.	
Road	0,4,6,8	500 m,1000 m	For major roads and highways, areas within a 1000-m impact range are assigned a maximum score of 8. Areas within a 500-m impact range of secondary roads and trunk roads receive 6 points, while areas within a 500-m impact range of other minor roads are assigned 4 points. Areas without roads receive 0 points.	Arias-Patino et al. (2024) and Liu et al. (2023b)
Railway	0,8	1000 m	For railways, areas within a 1000-m impact range are assigned a maximum score of 8, while areas without railways receive 0 points.	

StandardScaler, and missing values are imputed. The model's predictions are then reconstructed into their original spatial format, considering overlaps to ensure seamless integration.

Additionally, the model applies constraints to ensure that predicted values are non-negative, reflecting the realistic conditions of GDP, NL, PopD, and GI. Using historical data and these sophisticated preprocessing and training techniques, the MLP effectively learns the patterns and trends, enabling accurate predictions for future years on the QXP.

3.6. Accuracy verification

The Kappa coefficient and overall accuracy (OA) were calculated using a confusion matrix with a sampling rate of 0.10 additionally (Yu et al., 2024a, 2024b; Jian et al., 2024). The calculation methods are as follows (Eqs. (7) and (8)).

$$OA_o = \frac{\sum_{k=1}^{n} OA_{kk}}{N} \tag{7}$$

$$Kappa = \frac{OA_O - OA_E}{(1 - OA_E)} \tag{8}$$

where OA_o is the overall accuracy, OA_E is the probability of chance agreement between the simulated and actual results, and OA_{kk} represents the number of samples correctly identified for land use type k.

Since GDP, PopD, NL, and GI data represent intensity values rather than categorical data like LULC, OA is more appropriate for these intensity values. OA directly reflects the consistency between predicted and actual values, while the Kappa statistic is mainly used to assess the accuracy of categorical data classification and thus cannot adequately capture the accuracy characteristics of continuous data. Therefore, in the accuracy validation process, this study uses the OA metric to validate the accuracy of GDP, PopD, NL, and GI data (Supplementary II).

4. Results and analysis

4.1. Historical evolution of habitat indicators and risk of the QXP from 2000 to 2020

4.1.1. Land use and land cover (LULC) changes

From 2005 to 2010, the meadowland experienced substantial degradation, with an area reduction of 227,680 km^2, representing −15.84 % of the total meadow area. Concurrently, forest and water lands were expanded by 39,535 km^2 (14.65 %) and 19,140 km^2 (18.16 %), respectively. These transformations were predominantly observed in the southwestern region of the QXP (Fig. 3; Supplementary Fig. 1). The significant reduction in the meadow area, which far exceeded the combined increase in forest and water areas, suggested a potential issue of overgrazing and desertification in the region. In the remaining period, from 2000 to 2005 and after 2010, the areas of different habitat types remained unchanged.

From 2005 to 2010, the meadowland experienced substantial degradation, with an area reduction of 227,680 km^2, representing −15.84 % of the total meadow area. Concurrently, forest and water lands were expanded by 39,535 km^2 (14.65 %) and 19,140 km^2 (18.16 %), respectively. These transformations were predominantly observed in the southwestern region of the QXP (Supplementary Fig. 1). The significant reduction in meadow area, which far exceeded the combined increase in forest and water areas, suggested a potential issue of overgrazing and desertification in the region. In the remaining period, from 2000 to 2005 and after 2010, the areas of different habitat types remained unchanged.

Compared to habitats, the stressors of town land and plowland are relatively more minor, but both exhibit a clear growth trend (Supplementary Fig. 2). From 2005 to 2010, the area of plowland increased by 2908 km^2 (12.04 %), while the area of town land expanded by 283 km^2 (18.55 %) from 2000 to 2005, by 573 km^2 (31.71 %) from 2005 to 2010, and by 529 km^2 (22.25 %) from 2010 to 2015 (Table 3).

4.1.2. The stressor of HFI and GI

In addition to the previously discussed plowland and town land, key economic and demographic factors such as GDP, PopD, NL, and the

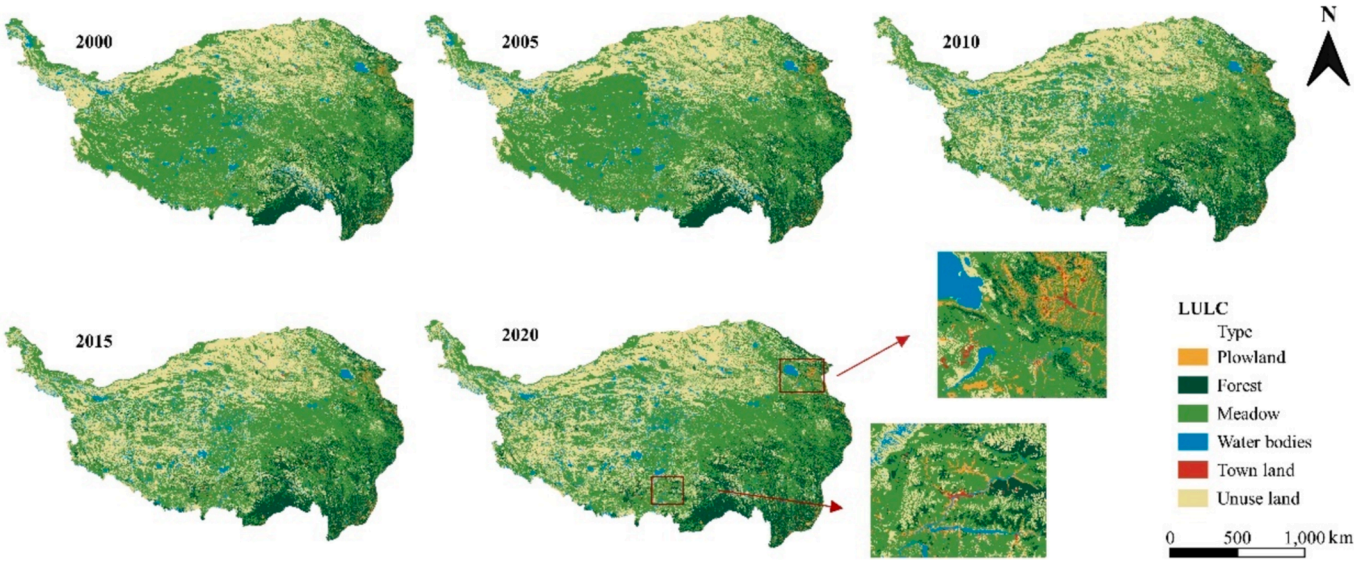

Fig. 3. Spatial and temporal changes in LULC on the QXP from 2000 to 2020.

Table 3
The area of LULC and change rate in 2000–2020 (km^2).

Type	2000	2005	2010	2015	2020
Meadow (Change rate)	1,437,657	1,436,997 (−0.05 %)	1,209,317 (−15.84 %)	1,208,725 (−0.05 %)	1,209,244 (0.04 %)
Forest (Change rate)	269,514	269,802 (0.11 %)	309,337 (14.65 %)	309,659 (0.10 %)	309,197 (−0.15 %)
Lake (Change rate)	104,697	105,422 (0.69 %)	124,562 (18.16 %)	124,902 (0.27 %)	130,641 (4.60 %)
Plowland (Change rate)	24,374	24,147 (−0.93 %)	27,055 (12.04 %)	26,926 (−0.48 %)	26,783 (−0.53 %)
Town land (Change rate)	1523	1806 (18.55 %)	2379 (31.71 %)	2908 (22.25 %)	2917 (0.31 %)

extent of road and railway networks were incorporated into the HFI assessment (Supplementary Fig. 3). From 2000 to 2020, the HFI on the QXP witnessed an increase predominantly within the eastern and southern sectors characterized by advanced transportation infrastructure (Fig. 4).

Grazing areas were predominantly concentrated from the northeastern to the southwestern sections of the meadow areas. GI on the northeastern and southwestern margins of the QXP demonstrated a consistent decline, indicative of a potential reduction in livestock pressure or changes in grazing management practices over time (see Fig. 5). Conversely, GI within the interior regions exhibited a contrasting upward trend, indicating that human utilization of vegetation areas in meadows and alpine meadows is intensifying (Fig. 4).

4.1.3. *Historical habitat risk assessment results and temporal changes*

From 2000 to 2020, the habitat risk significantly changed across different levels (Fig. 6; Table 4). According to the data, the low-risk areas experienced a significant decrease between 2005 and 2010 (a decline of 13.64 %), followed by a slight rebound (an increase of 3.93 %). However, the overall trend remains downward, indicating that relatively safe habitats are shrinking. At the same time, the medium-risk and high-risk areas saw a notable increase in 2005, with growth rates of 31.74 % and

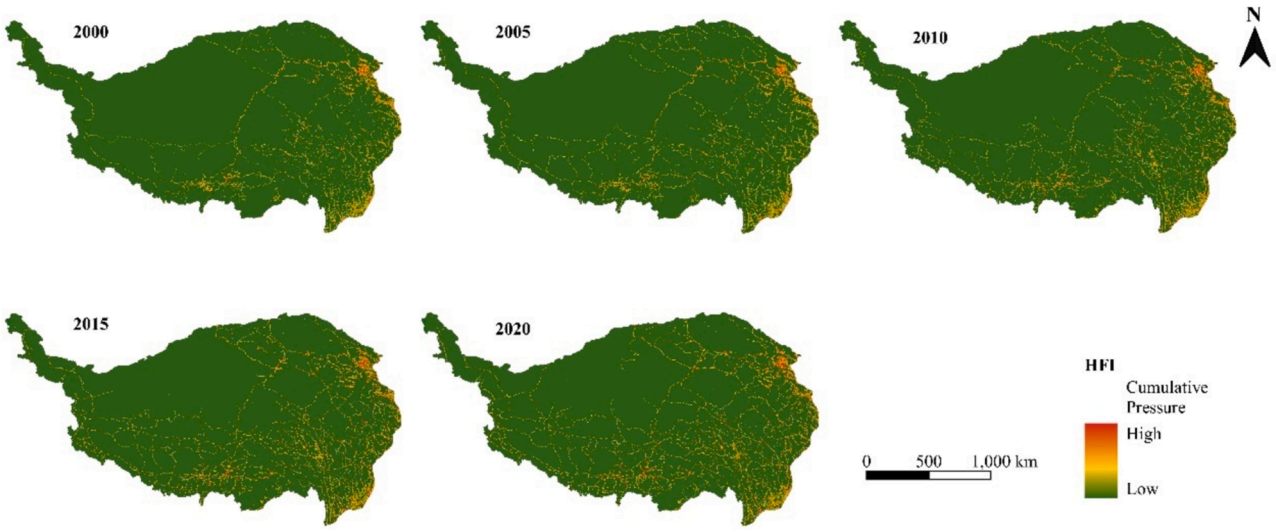

Fig. 4. Spatial and temporal changes in HFI on the QXP from 2000 to 2020. The localized area is where the changes in the "HFI" are more evident.

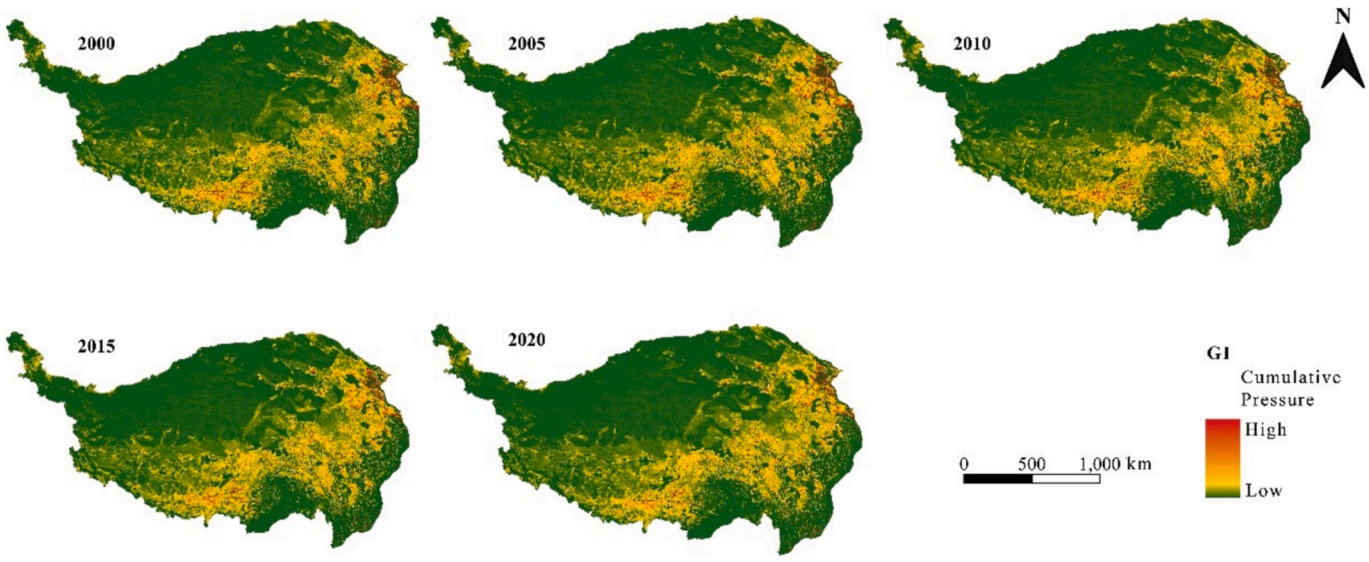

Fig. 5. Spatial and temporal changes in GI stressors on the QXP from 2000 to 2020.

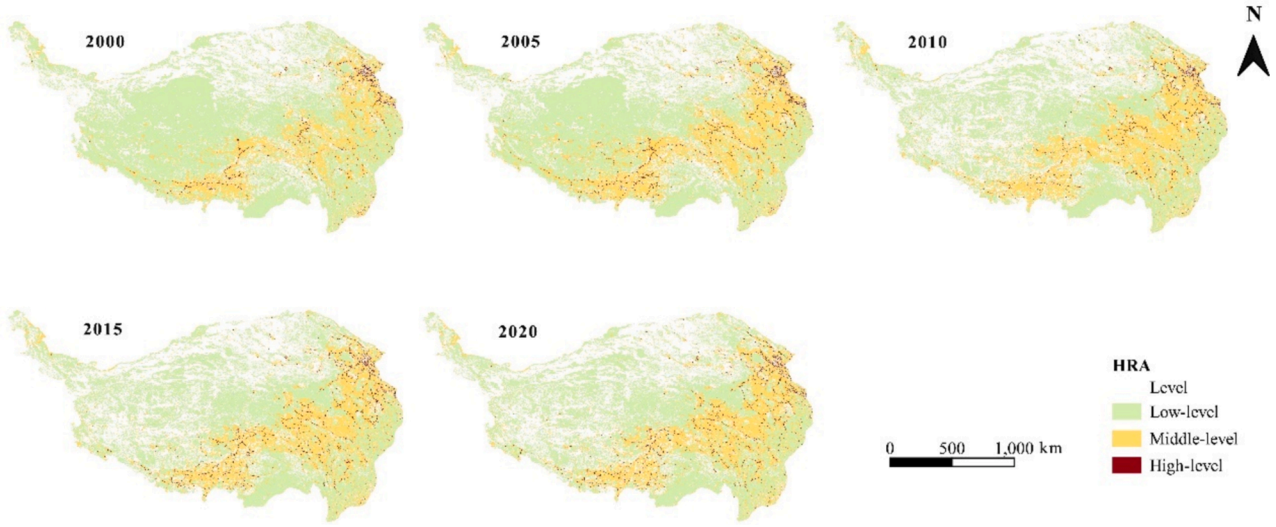

Fig. 6. Spatial and temporal variation in ecosystem habitat risk on the QXP from 2000 to 2020.

Table 4
The area of habitat risk and change rate in 2000–2020 (km^2).

Level	2000	2005	2010	2015	2020
Low-level (Change rate)	23,411,689	21,120,105 (−9.79 %)	18,237,989 (−13.64 %)	18,954,743 (3.93 %)	18,879,792 (−0.40 %)
Middle-level (Change rate)	6,783,716	8,936,014 (31.74 %)	9,050,741 (1.29 %)	8,235,582 (−9.00 %)	8,377,926 (1.73 %)
High-level (Change rate)	369,366	514,625 (39.32 %)	431,029 (−16.22 %)	530,606 (23.11 %)	560,982 (5.72 %)

39.32 %, respectively. It reflects the expansion of human activities during this period, particularly urbanization, agricultural land expansion, and infrastructure development. However, from 2005 to 2010, the growth rate of medium-risk areas slowed, and the high-risk areas saw a 16.22 % decrease, suggesting that policy interventions began to take effect, curbing the expansion of middle and high risk areas.

4.2. Prediction of future habitat indicators

4.2.1. Simulation of future LULC in multiple scenarios

The PLUS model was applied to predict future land use changes (Supplementary Figs. 4 and 5). The BAU scenario projection is consistent with the observed LULC trends from 2000 to 2020, which indicates an overall decreasing trend for meadow and water body areas, in contrast to the increasing trend for forest areas. Projections for 2025 and 2035 under the BAU scenario indicate a continued decline in meadow and water areas, while forest coverage is expected to expand further. The EP scenario underscores a pronounced emphasis on environmental conservation in stark contrast to the BAU scenario. It projects a significant increase in forest areas and continuous growth for meadows and water areas throughout the projection period from 2025 to 2035. Conversely, the town land area initially decreases but slightly increases from 2030 to 2035. The area of plowland land is consistently projected to decline, while the area of unused land is anticipated to reduce substantially.

Under the UD scenario, LULC exhibits distinctive characteristics. The area of plowland shows an increase by 2025 and then remains unchanged. Forest and meadow areas experience a gradual decline over the projected period from 2025 to 2035. In contrast, water areas display a slight but steady increase. Town land areas show significant growth, while the area of unused land remains relatively stable with a slight increase (Fig. 7; Table 5).

4.2.2. Prediction of HFI and GI based on MLP

4.2.2.1. HFI prediction. As for HFI, in the BAU scenario, the area of regions with no HFI gradually decreases, while areas with lower level HFI show an increasing trend. Areas with higher levels of HFI remain relatively stable. In the EP scenario, the area of regions lacking HFI also declines, although the growth rates of areas with lower HFI are comparatively slower. Changes in areas with high HFI are relatively stable. In the UD scenario, the area of regions with no HFI experiences the most significant decrease, and areas with lower HFI exhibit the fastest growth rates. Changes in areas with high HFI are like other scenarios but indicate tremendous pressure on the ecosystem due to increased population density and infrastructure expansion (Fig. 8; Supplementary Fig. 6).

4.2.2.2. GI prediction. From 2025 to 2035, the GI exhibits distinct trends across the scenarios. In the BAU scenario, areas with no GI show a relatively stable trend with slight fluctuations over time. Low GI areas gradually decrease initially but stabilize towards the end of the period. Middle GI areas experience an increase followed by a slight decline, while high GI areas steadily increase throughout the period. Under the EP scenario, areas with no GI show an initial increase followed by a decrease, with an upward trend. Areas with low GI initially decrease but recover towards the end of the projection period. Middle and high GI areas show continuous decreases or minor fluctuations, reflecting conservation efforts and sustainable grazing practices. In the UD scenario, the area with no GI remains relatively stable with minor fluctuations. Low GI areas decrease gradually, while medium and high GI areas exhibit modest increases followed by slight decreases or stable patterns (Fig. 9).

4.3. Habitat risk assessment under multiple scenarios

The study calculates the habitat stressors to the QXP from plowland expansion, urbanization, grazing pressure, and human footprint pressures for 2025–2035 under three scenarios. Examining three distinct scenarios delineates the spatial distribution of overall habitat risk across the QXP (Fig. 10; Table 6).

4.3.1. Comparison of time series of habitat risk areas

Overall, the habitat risk trends under the BAU scenario remain relatively stable, aligning with the trends observed from 2000 to 2020. It suggests that future habitat risks will continue without significant policy interventions. In contrast, the EP scenario demonstrates that with intense policy interventions, habitat risks can be effectively mitigated, particularly evidenced by the continuous reduction of high-risk areas and the significant expansion of low-risk areas, underscoring the effectiveness of ecological protection measures. On the other hand, the UD scenario highlights the rapid escalation of habitat risks driven by increased human activity, urban land expansion, and agricultural land use. Expanding medium- and high-risk areas will intensify without appropriate policy measures, putting further pressure on ecosystems.

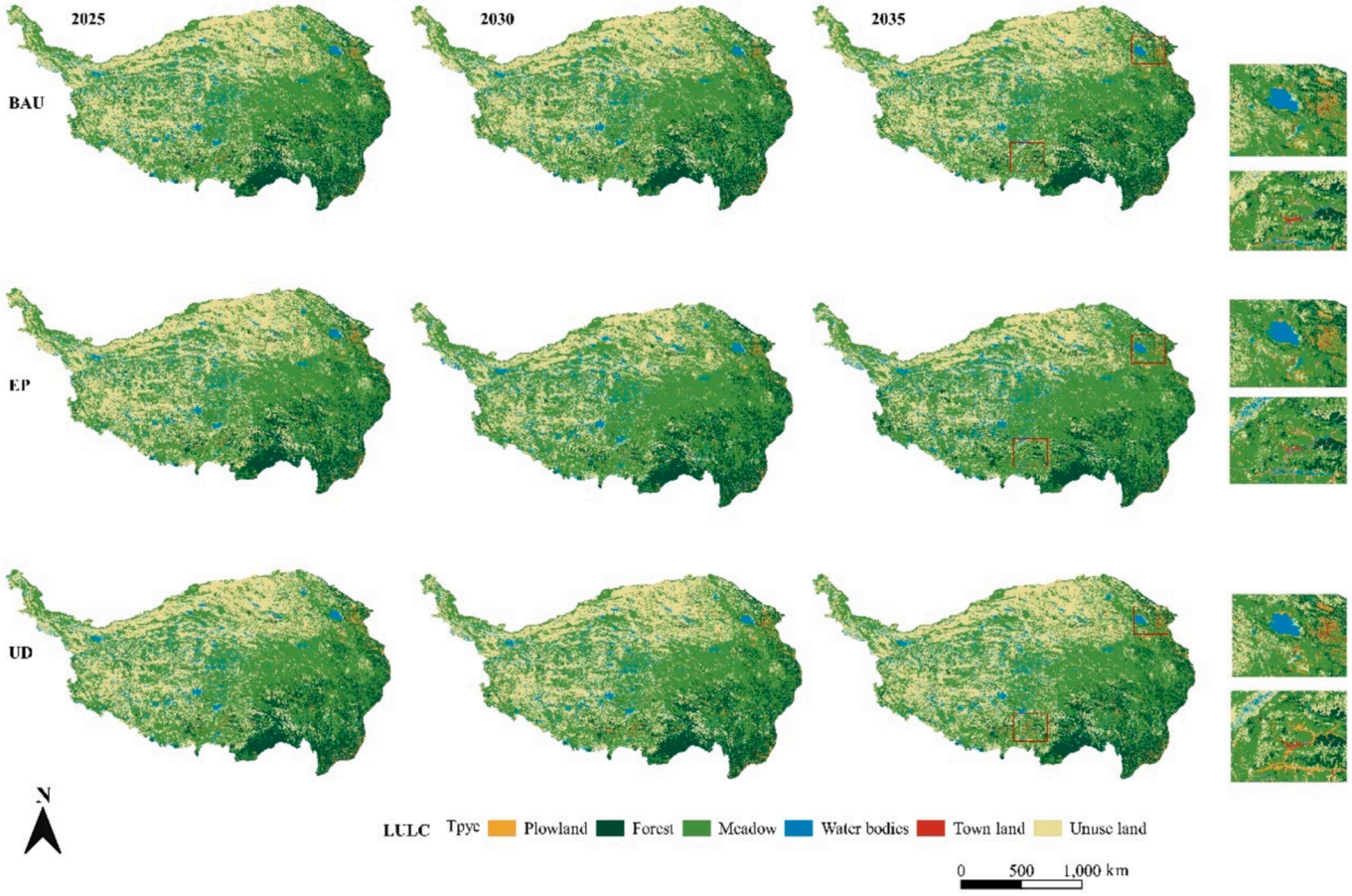

Fig. 7. Simulation of LULC in multiple scenarios on the QXP from 20,250 to 2035.

Table 5
The area of LULC and change rate in 2025–2035 under multi-scenario (km^2).

Scenarios	Type	2025	2030	2035
BAU	Plowland (Change rate)	27,229 (1.67 %)	27,288 (0.21 %)	25,648 (−6.01 %)
	Forest (Change rate)	309,390 (0.06 %)	309,459 (0.02 %)	309,509 (0.02 %)
	Meadow (Change rate)	1,208,924 (−0.03 %)	1,208,572 (−0.03 %)	1,208,125 (−0.04 %)
	Water (Change rate)	119,271 (−8.70 %)	114,790 (−3.76 %)	111,247 (−3.09 %)
	Town (Change rate)	3061 (4.95 %)	3334 (8.89 %)	3438 (3.13 %)
	Unuse (Change rate)	832,122 (1.34 %)	836,496 (0.53 %)	841,970 (0.65 %)
EP	Plowland (Change rate)	24,098 (−10.02 %)	23,495 (−2.50 %)	21,711 (−7.60 %)
	Forest (Change rate)	311,026 (0.59 %)	330,640 (6.31 %)	341,330 (3.23 %)
	Meadow (Change rate)	1,251,492 (2.66 %)	1,351,410 (8.85 %)	1,391,947 (3.00 %)
	Water (Change rate)	134,390 (2.87 %)	142,279 (5.87 %)	151,171 (6.25 %)
	Town (Change rate)	2755 (−5.53 %)	2414 (−12.37 %)	2439 (1.01 %)
	Unuse (Change rate)	786,176 (−4.26 %)	649,700 (−17.36 %)	591,340 (−8.98 %)
UD	Plowland (Change rate)	28,830 (7.63 %)	29,102 (0.94 %)	29,015 (−0.30 %)
	Forest (Change rate)	308,707 (−0.16 %)	308,114 (−0.19 %)	307,521 (−0.19 %)
	Meadow (Change rate)	1,207,653 (−0.11 %)	1,206,767 (−0.10 %)	1,205,582 (−0.10 %)
	Water (Change rate)	123,548 (−5.42 %)	123,869 (0.26 %)	124,548 (0.55 %)
	Town (Change rate)	3272 (12.17 %)	3564 (19.85 %)	4157 (16.63 %)
	Unuse (Change rate)	827,929 (0.83 %)	828,522 (0.07 %)	829,114 (0.07 %)

Specifically, In the BAU scenario, low-risk areas exhibit a gradual decline. Middle-risk areas will expand significantly between 2020 and 2025 (15.09 %), and although the growth rate will slow after 2030, a stable upward trend persists overall. High-risk areas show notable volatility, with a sharp decrease from 2020 to 2025 (−12.83 %) and a marked rebound after 2030 (13.90 %), suggesting that expanding high-risk areas could pose potential environmental challenges. In the EP scenario, low-risk areas demonstrate the most significant change, particularly from 2025 to 2030, with a substantial increase (16.38 %). Middle-risk areas exhibit considerable fluctuations. In contrast, high-risk areas undergo a sharp reduction between 2020 and 2025 (−77.60 %), underscoring the effectiveness of protective measures in curbing high-risk zones. The UD scenario shows the most drastic changes in risk distribution. Low-risk areas sharply contract in the initial period (−17.79 %), reflecting intense urban encroachment. Simultaneously, middle-risk areas experience rapid expansion between 2020 and 2025 (31.10 %), followed by relative stability. The expansion of high-risk areas is particularly striking, dramatically increasing from 2020 to 2025 (99.97 %). Although the growth slows between 2025 and 2030, the overall trend of substantial expansion continues, highlighting the significant pressure urbanization exerts on the ecological environment.

4.3.2. *Comparison of regional scenarios of habitat risk*

Using the BAU scenario as a reference, a comparison of the EP and UD scenarios reveals that the ecological protection policies in the EP scenario effectively curtail the expansion of high-risk areas. In contrast, urban expansion in the UD scenario exerts substantial environmental pressure, particularly in expanding high-risk areas. The detailed analysis is as follows:

By 2025, compared to the BAU scenario, the EP scenario shows an increase of 6.55 % in low-risk areas, minimal change in medium-risk areas, and a significant reduction of 74.30 % in high-risk areas. In contrast, the UD scenario exhibits a significant decrease of 11.27 % in

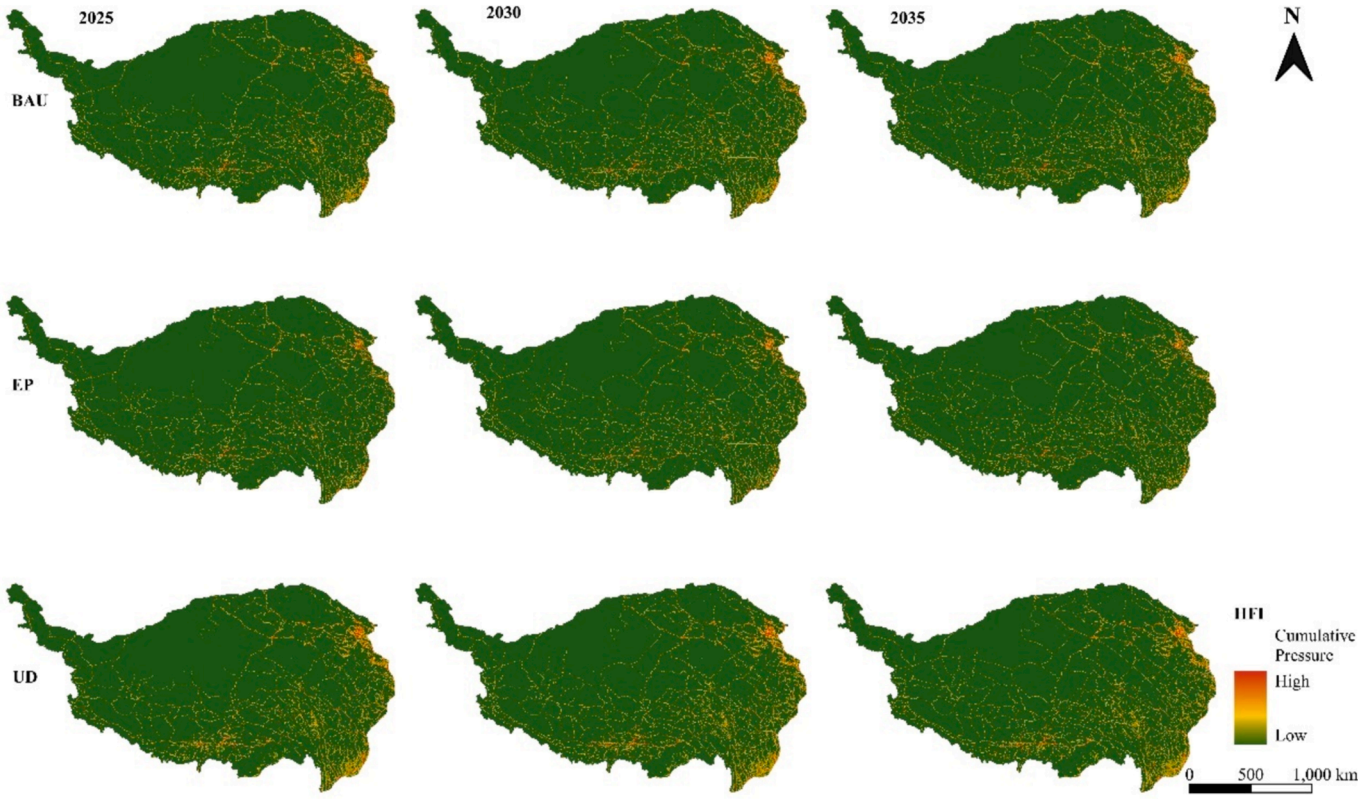

Fig. 8. Simulation of HFI in multiple scenarios.

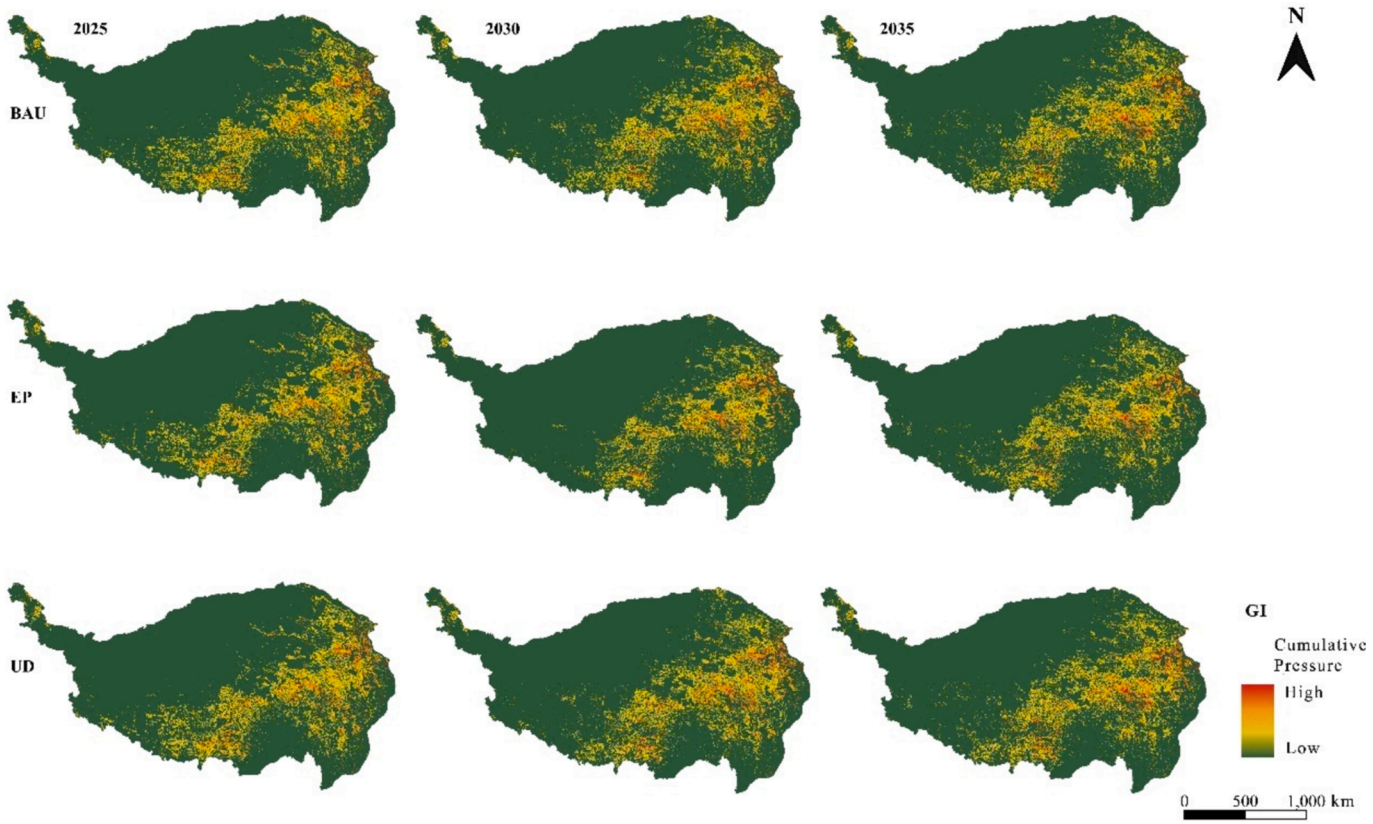

Fig. 9. Simulation of GI in multiple scenarios.

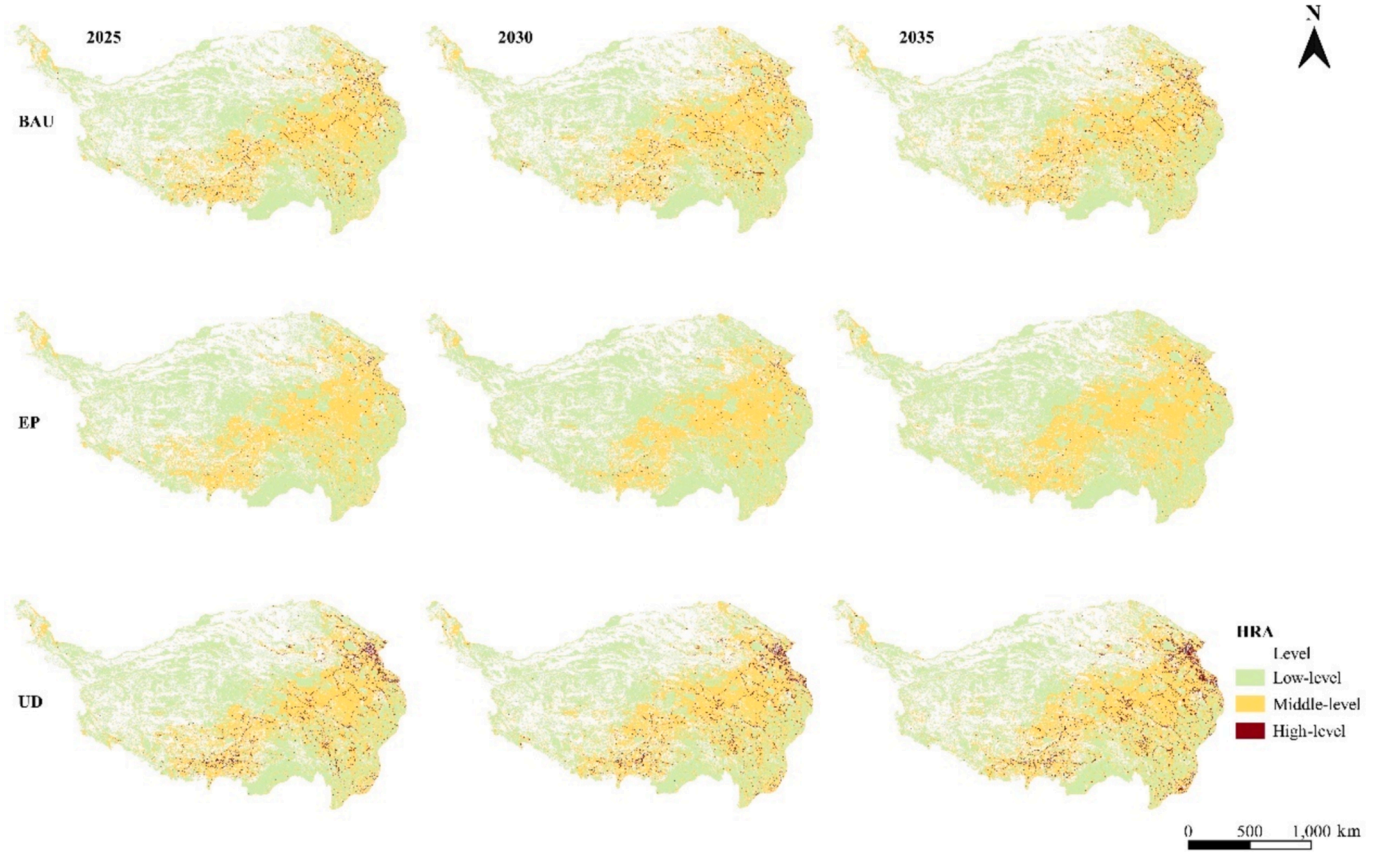

Fig. 10. Simulation of habitat risks in multiple scenarios.

Table 6
The area of habitat risks and change rates in 2025–2035 under multi-scenario (km^2).

Scenarios	Type	2020	2025	2030	2035
BAU	Low-level risk (Change rate)	18,879,792	17,493,224 (−7.34 %)	16,654,554 (−4.79 %)	16,378,270 (−1.66 %)
	Middle-level risk (Change rate)	8,377,926	9,642,507 (15.09 %)	10,395,330 (7.81 %)	10,540,090 (1.39 %)
	High-level risk (Change rate)	560,982	489,017 (−12.83 %)	491,295 (0.47 %)	559,573 (13.90 %)
EP	Low-level risk (Change rate)	18,879,792	18,638,191 (−1.28 %)	21,690,859 (16.38 %)	20,951,050 (−3.41 %)
	Middle-level risk (Change rate)	8,377,926	9,692,924 (15.70 %)	8,977,838 (−7.38 %)	10,729,493 (19.51 %)
	High-level risk (Change rate)	560,982	125,688 (−77.60 %)	106,276 (−15.44 %)	108,607 (2.19 %)
UD	Low-level risk (Change rate)	18,879,792	15,520,769 (−17.79 %)	15,849,637 (−2.12 %)	15,520,769 (−2.07 %)
	Middle-level risk (Change rate)	8,377,926	10,983,314 (31.10 %)	10,902,086 (−0.74 %)	10,983,314 (0.75 %)
	High-level risk (Change rate)	560,982	1,121,790 (99.97 %)	892,695 (−20.43 %)	1,121,790 (25.66 %)

low-risk areas, a substantial increase of 13.91 % in medium-risk areas, and a dramatic expansion of 129.38 % in high-risk areas.

By 2030, the EP scenario shows a 30.24 % increase in low-risk areas compared to the BAU scenario, a decrease of 13.63 % in medium-risk areas, and a significant reduction of 78.36 % in high-risk areas. In comparison, the UD scenario shows minimal changes in low and medium-risk areas, with a dramatic expansion of 81.70 % in high-risk areas. In 2035, the EP scenario shows a 27.92 % increase in low-risk areas compared to the BAU scenario, minimal change in medium-risk areas, and a significant reduction of 80.59 % in high-risk areas. Conversely, the UD scenario shows minimal changes in low and medium-risk areas, while high-risk areas experience a dramatic expansion of 100.47 %.

5. Discussion

5.1. Habitat risk assessment dynamics and temporal changes on the QXP

Between 2000 and 2020, the HFI showed a steady upward trend, with the main areas of growth concentrated around urban centers and transportation networks. This trend was closely related to infrastructure development, particularly the expansion and improvement of roads, railways, and urban areas. In these highly active regions, agricultural expansion, industrial development, and residential construction exerted significant pressure on local ecosystems, potentially leading to reductions in biodiversity and degradation of ecosystem services (Correa-Ayram et al., 2017). Overall, the spatial distribution and trends of HFI significantly impacted the ecological environment and sustainable development of the QXP. Future conservation and development strategies must have considered the effects of HFI on ecosystems, implementing appropriate measures to balance economic growth with environmental protection, especially in ecologically sensitive and biodiversity-rich areas.

Since meadows played a crucial role in carbon sequestration, overgrazing may have weakened this ecological service, exacerbating the adverse effects of climate change (Song et al., 2009; Li et al., 2024). In meadow regions, the increase in GI similarly contributed to the degradation of ecosystem services, particularly in terms of water retention capacity and soil quality (Liu et al., 2022). Meadow ecosystems typically supported high levels of biodiversity, but overgrazing could alter the composition of plant communities, which in turn affected the overall structure and function of the ecosystem. The rising grazing intensity placed considerable pressure on the ecological environment of the QXP. Future management strategies must have considered balancing GI with ecological protection to ensure that this globally significant ecological region continued to provide essential ecosystem services while conserving its biodiversity.

Over the past two decades, the QXP predominantly featured low-risk habitats, which were concentrated mainly in the central alpine meadows and southern tropical rainforests, often situated within the protective confines of nature reserves (Fig. 6; for specific distribution, see Supplementary Fig. 7). These regions exhibit by low GI and minimal human disturbance, contributing to their lower threat status. In contrast, high-risk zones are predominantly found in the eastern temperate meadows and broadleaf forests, where higher GI, human activity, and urbanization pressures result in considerable anthropogenic interference. Middle-risk areas are typically located at the transition zones between low- and high-risk regions, creating a gradient of risk levels (Zhang et al., 2023).

During this period, 2005 was a critical turning point for habitat risk, with middle and high habitat risk areas significantly increasing (31.74 % and 39.32 %, respectively). This shift was mainly due to China's rapid urbanization process. From 2000 to 2005, urban expansion and infrastructure development peaked, with the rapid expansion of highways, rail networks, and large-scale urbanization driving dramatic changes in land-use patterns (Correa-Ayram et al., 2017; Munthali et al., 2023). Particularly in ecologically fragile areas like the QXP, infrastructure projects (such as the Qinghai-Xizang Railway) promoted regional economic development and greatly intensified human activity. However, these construction activities substantially negatively impacted the ecosystem during this period, leading to habitat fragmentation, loss of natural habitats, and degradation of ecological functions (Zhang et al., 2023; Liu et al., 2023b; Cui et al., 2022). Due to the intrinsic fragility and weak recovery ability of plateau ecosystems, the surge in high-risk areas in 2005 reflects the intense ecological pressure brought by urbanization and infrastructure development during this period.

The initial phase from 2020 to 2025 shows a notable increase in the transition to higher risk categories, signaling potential environmental challenges ahead. To address growing ecological pressures, the Chinese government has progressively implemented stricter protection policies on the QXP. For example, the Sanjiangyuan Nature Reserve Project launched in 2005. Major plans such as the "Xizang Ecological Security Barrier Protection Plan (2008–2030)" and the "Qinghai-Xizang Plateau Ecological Construction Plan (2011–2030)" further strengthened conservation efforts. The implementation of these policies has led to complex changes in habitat risks on the QXP. The government's protective measures have significantly reduced ecological pressure in certain areas. However, as economic development and urbanization continue to advance, habitat risks in some regions remain on the rise, reflecting the ongoing threat that human activities pose to fragile ecosystems.

5.2. Future habitat risk trend

In future scenario analyses, the BAU scenario maintains the continuity of current development and protection policies and predicts that low habitat risk areas in QXP will decrease between 2020 and 2035 due to escalating human activities and urban expansion. Initially, middle habitat risk areas are expected to expand significantly, with their growth stabilizing later, while high habitat risk areas are projected to fluctuate. This overall trend aligns with the changes in habitat risk areas observed from 2000 to 2020. The EP and UD scenarios present development trajectories that differ from the BAU scenario. The area of high habitat risk in the EP scenario decreased by more than 74 % in each period. In contrast, the area of high habitat risk in the UD scenario increased by more than 81 %.

Several key factors influence these variations significantly in the

context of spatial and temporal changes in habitat risk on the QXP from 2025 to 2035. Policy enforcement intensity emerges as the predominant factor across all considerations (Liang & Song, 2022). Particularly in the UD scenario, relaxed environmental protection policies lead to a substantial transformation of moderate-risk habitats into high-risk ones. Over the past 20 years, forest habitats on the QXP have increased, with stability achieved after 2010, likely influenced by national forest protection projects and ecological compensation policies. Water body habitats have also slightly increased, reflecting the effectiveness of national wetland protection measures. However, the growth in construction land and the acceleration of urbanization poses challenges, potentially leading to land resource consumption and environmental degradation (Liu et al., 2023a).

In 2023, China enacted the "Qinghai-Xizang Plateau Ecological Protection Law," setting basic principles for ecological protection and outlining measures such as improving management, ensuring ecological safety, enhancing protection and restoration, and strengthening risk prevention and supervision (Qiushi, 2023). The law specifies protection for critical ecosystems like rivers, lakes, grasslands, forests, and wetlands, focusing on areas like the Sanjiangyuan region. It also mandates protection for rare and endangered species native to the plateau. The law promotes sustainable development by advocating for farmland conservation, desertification control, soil erosion prevention, and green mining practices.

Regionally, Gansu's northern part is crucial for national sand prevention, while its southwest is an essential ecological barrier. The eastern and southeastern parts of the plateau are part of the Qinghai-Xizang Plateau-Sichuan-Yunnan ecological shield, highlighting Gansu's role in windbreak and sand fixation, water source conservation, and soil and water retention. Qinghai is poised to become a national ecological security and conservation area, supporting the "Belt and Road" initiative. Xizang focuses on sustainable development for high-quality growth. Yunnan aims to lead in ecological civilization and serve as a South and Southeast Asia hub.

Considering ecological protection policies and spatial planning, the EP scenario reflects a realistic QXP future. It is achieved through stringent regulations on land conversion, protecting nature reserves, and expanding ecological lands, thereby fortifying ecosystem resilience. These interventions diminish the short-term expanse of middle- and high-risk areas, transforming them into low-risk areas. The enduring impact of these strategies is also apparent in the long term, showcasing their efficacy in mitigating habitat risks. The initial stages of implementation have seen a substantial shift from medium- to low-risk areas, with a notable decrease in high-risk zones. This transformation underscores the effectiveness of ecological protection measures in curbing habitat risk by reducing the extent of medium- to high-risk areas and expanding the low-risk landscape (Xue et al., 2023). On the contrary, the UD scenarios exhibit poor risk control, with a clear potential for increased risk. This comparison indicates the detrimental effects of urbanization on ecosystems and underscores the critical importance of ecological protection strategies. Consequently, these strategies are proven to be highly effective in reducing habitat risk on the QXP, not only in the short term but also in demonstrating long-term stability.

5.3. Policy implications

Our examination of the ramifications of policies on prospective habitats reveals a trend that priority for land use policies always results in sacrificing plowland rather than ecological land. This inclination stands in contrast to findings from research conducted on Hainan Island (Zhang et al., 2024) and Wuhan (Ke et al., 2018) yet is consistent with the study on Guizhou Province (Guo et al., 2023a, 2023b). Such variance in the policy-driven outcomes underscores an intensified focus on ecological stewardship, particularly in the regions of western China with high vegetation coverage rates but less developed. This heightened emphasis on conservation underscores the strategic importance of safeguarding these areas, which are often the custodians of rich biodiversity and critical ecosystem services.

This study has argued that the EP scenario best encapsulates a plausible future trajectory for the QXP. In the future, stringent policies for conserving grasslands, forests, and water bodies will enhance ecosystem resilience (Li et al., 2022). However, there is a potential shift towards economic development as a priority once the ecological environment reaches a certain threshold of improvement. It is particularly plausible in regions with superior ecological conditions and minority ethnic populations, especially those with higher vegetation cover, favorable climates, and proximity to economically vibrant Sichuan Province and Yunnan Province, where the demand for economic advancement is more pronounced, and the environmental impact of human activities is relatively subdued (Wang et al., 2023a, 2023b).

In its pursuit of robust ecological protection and sustainable development, the Chinese government has strategically delineated ecological red lines in recent years (Hu et al., 2022; Gu et al., 2023; Zeng et al., 2024). This initiative is pivotal, covering more than half of the QXP within protective boundaries. The goal is to safeguard areas of vital ecological importance on the plateau, ensuring the conservation of their inherent functions, preventing any reduction in area, and preserving their essential characteristics (Liu and Chen, 2023; Nie et al., 2023). While the protection within the red line regions is less stringent than in nature reserves, allowing certain socio-economically valuable activities, the ecological red line policy is a cornerstone of regional ecological conservation.

Our predictive results indicate that, even with the ecological red line policy in place, specific areas within the central QXP, especially in the southern regions of Qinghai Province, may face increased habitat risks by 2035 (Fig. 10; for specific distribution, see Supplementary Fig. 8). This forecast highlights the unwavering need for a steadfast commitment to ecological conservation strategies. It also emphasizes the ongoing efforts to protect our natural environments for future generations. The ecological red line policy represents a balanced approach that integrates conservation with sustainable development, setting a precedent for other regions grappling with similar ecological challenges.

Moreover, the QXP can sensibly establish objectives for expanding built-up land. An emphasis on a particular land use type can precipitate a significant alteration in ecosystem services (Guo et al., 2023a, 2023b). Under precise delineation and stringent conservation measures, these regions can judiciously expand built-up areas to accommodate economic development. Concurrently, we have identified spatial conflicts between environmental preservation and other land uses, a phenomenon prevalent in numerous locales and anticipated to be resolved through the holistic recalibration of Territorial Spatial Planning. Our framework offers an additional layer of guidance from a simulation-based perspective. The EP and UD scenarios illustrate two such contrasting extremes. It serves as a reminder that urban expansion and greening initiatives must be meticulously deliberated to ensure a balanced approach.

5.4. Limitation and future work

This study integrated multiple models, including InVEST, PLUS, and MLP, to design a comprehensive framework for analyzing the spatio-temporal variations of habitat risk on the QXP under multiple scenarios. This innovative approach combines GI, HFI, and LULC data to advance the prediction of habitat risk within the QXP. However, our study encounters certain limitations.

The scarcity of historical data for training the multilayer perceptron network restricts the model's predictive scope to a 15-year horizon, precluding the possibility of long-term projections. Additionally, external factors such as policy shifts, climatic uncertainties, and economic instabilities may compromise the predictive accuracy, potentially causing discrepancies in future outcomes.

Moreover, the three scenarios utilized in this analysis may not

encapsulate the full spectrum of real-world transformations. The presuppositions regarding future developments might not wholly mirror reality's intricate and fluid character. Consequently, further inquiry is imperative to refine these scenarios, ensuring that our simulations are more reflective of genuine environmental and socio-economic dynamics.

6. Conclusions

In this study, we assessed the conservation effectiveness of policy formulation on the QXP by examining habitat risk assessment and forecasting in multi-scenario simulations. The separated indicators HFI and GI are introduced into the evaluation and prediction framework of human activities, aiming to capture the unique ecological challenges faced by the plateau more accurately. We integrate multiple models to construct a multi-scenario habitat risk prediction framework based on InVEST-PLUS-MLP, fully considering development needs and diverse predictive factors, thus providing more accurate scientific support for future policymaking.

From 2000 to 2020, the QXP observed a significant contraction in meadow lands, juxtaposed with a notable expansion in forest and water body areas. However, these individual gains were overshadowed by an overall reduction in the total habitat area. These transformations highlight the pressing challenges faced in the region's environmental stewardship. The scenario simulation results show that, under the EP scenario, the area of high-risk zones decreased by more than 74 % per period compared to the BAU scenario from 2025 to 2035. In contrast, in the UD scenario, the area of high-risk zones increased by more than 81 %. In the BAU scenario, land use types have undergone stable and moderate changes. grazing intensity and the human footprint index both show relatively stable trends, and habitat risk assessment have also maintained a relatively stable state. The magnitude of ecological environmental changes is small, maintaining the current balance. In the EP scenario, the areas of forests and meadows significantly increased. Both low and high grazing intensity areas have significantly decreased. The significant increase in low-level habitat risk areas indicates that more habitats have been improved and restored, while the reduction in high-level habitat risk areas suggests that high-risk areas have been effectively controlled and protected. In the UD scenario, urban agglomeration levels continuously improve, and urban utilization rates steadily increase, while high-level habitat risk areas significantly increase. Urban expansion exerts greater pressure on ecosystems. The habitat risks posed by urbanization remain a concern.

We argue that the EP scenario will likely be the most probable development path for QXP, focusing on robust conservation measures to safeguard grasslands, forests, and water bodies, thereby bolstering the ecosystem's resilience. Even under the stringent environmental protection scenario, there will be a trend of increasing habitat risk in the central and eastern regions of the QXP. We advocate a balanced approach, acknowledging that while environmental protection is paramount, sustainable economic development should not be neglected. The QXP can sensibly establish objectives for the expansion of built-up land. When the ecological conditions have significantly improved and are on a stable trajectory, the strategic focus can be appropriately shifted to promoting economic growth.

CRediT authorship contribution statement

Farui Jiang: Writing – original draft, Visualization, Software, Methodology, Formal analysis, Data curation, Conceptualization. **Shaofen Xu:** Methodology, Data curation. **Chonghao Liu:** Writing – review & editing, Validation, Supervision, Investigation, Funding acquisition. **Jianan Zhao:** Software, Methodology. **Baode Jiang:** Writing – review & editing. **Fengyan Fan:** Writing – review & editing.

Declaration of competing interest

The authors declare that they have no known competing financial interests or personal relationships that could have appeared to influence the work reported in this paper.

Acknowledgments

The research was supported by the Second Tibetan Plateau Scientific Expedition and Research Program (Grant No. 2021QZKK0305) and the Basic Science Center Project of the National Natural Science Foundation of China (Grant No. 72088101). The National Tibetan Plateau/Third Pole Environment Data Center (http://data.tpdc.ac.cn) provides some data.

Appendix A. Supplementary data

Supplementary data to this article can be found online at https://doi.org/10.1016/j.ecolind.2024.112804.

Data availability

Data will be made available on request.

References

Arias-Patino, M., Johnson, C.J., Schuster, R., Wheate, R.D., Venter, O., 2024. Accuracy, uncertainty, and biases in cumulative pressure mapping. Ecol. Ind. 166, 112407. https://doi.org/10.1016/j.ecolind.2024.112407.

Arkema, K.K., Verutes, G.M., Wood, S.A., Clarke-Samuels, C., Rosado, S., Canto, M., et al., 2015. Embedding ecosystem services in coastal planning leads to better outcomes for people and nature. Proc. Natl. Acad. Sci. 112 (24), 7390–7395. https://doi.org/10.1073/pnas.1406483112.

Bai, L., Xiu, C., Feng, X., Liu, D., 2019. Influence of urbanization on regional habitat quality: a case study of Changchun City. Habitat Int. 93, 102042. https://doi.org/10.1016/j.habitatint.2019.102042.

Cabral, P., Levrel, H., Schoenn, J., Thiébaut, E., Mao. P.L., Rollet, C., et al., 2015. Marine habitats ecosystem service potential: a vulnerability approach in the Normand-Breton (Saint Malo) Gulf, France. *Ecosystem Services*, 16(Supplement C), 306–318. doi:10.1016/j.ecoser.2014.09.007.

Chen, J., Gao, M., Cheng, S., Hou, W., Song, M., Liu, X., 2022. Global 1 km × 1 km gridded revised real gross domestic product and electricity consumption during 1992–2019 based on calibrated nighttime light data. Sci. Data 9, 202. https://doi.org/10.1038/s41597-022-01322-5.

Chen, H., Ju, P., Zhang, J., Wang, Y., Zhu, Q., Yan, L., 2020a. Attribution analyses of changes in alpine grasslands on the Qinghai-Tibetan Plateau. Chin. Sci. Bull. 65 (22), 2406–2418. https://doi.org/10.1360/tb-2019-0619.

Chen, Z.Q., Yu, B.L., Yang, C.S., Zhou, Y.Y., Yao, S.J., Qian, X.J., et al., 2020b. An extended time-series (2000–2023) of global NPP-VIIRS-like nighttime light data. Harvard Dataverse. https://doi.org/10.7910/DVN/YGIVCD.

Chung, M.G., Kang, H., Choi, S.U., 2015. Assessment of Coastal Ecosystem Services for Conservation Strategies in South Korea. PLoS One 10 (7), e0133856.

Correa-Ayram, C.A., Mendoza, M.E., Etter, A., Pérez Salicrup, D., 2017. Anthropogenic impact on habitat connectivity: a multidimensional human footprint index evaluated in a highly biodiverse landscape of Mexico. Ecol. Ind. 72, 895–909. https://doi.org/10.1016/j.ecolind.2016.09.007.

Cui, P., Ge, Y., Li, S., Li, Z., Xu, X., Zhou, G., et al., 2022. Scientific challenges in disaster risk reduction for the Sichuan-Tibet Railway. Eng. Geol. 309, 106837. https://doi.org/10.1016/j.enggeo.2022.106837.

Drucker, D.G., Bridault, A., Cupillard, C., Hujic, A., Bocherens, H., 2011. Evolution of habitat and environment of red deer (Cervus elaphus) during the Late-glacial and early Holocene in eastern France (French Jura and the western Alps) using multi-isotope analysis (δ13C, δ15N, δ18O, δ34S) of archaeological remains. Quat. Int. 245 (2), 268–278. https://doi.org/10.1016/j.quaint.2011.07.019.

Duggan, J.M., Eichelberger, B.A., Ma, S., Lawler, J.J., Ziv, G., 2015. Informing management of rare species with an approach combining scenario modeling and spatially explicit risk assessment. Ecosyst. Health Sustain. 1 (6), 1–18. https://doi.org/10.1890/EHS14-0009.1.

Fetzel, T., Havlik, P., Herrero, M., Erb, K.H., 2017. Seasonality constraints to livestock grazing intensity. Glob. Chang. Biol. 23 (4), 1636–1647. https://doi.org/10.1111/gcb.13591.

Gu, Y., Lin, N., Cao, B., Ye, X., Pang, B., Du, W., et al., 2023. Assessing the effectiveness of Ecological Conservation Red Line for mitigating anthropogenic habitat degradation in river corridors. Ecol. Ind. 154, 110742. https://doi.org/10.1016/j.ecolind.2023.110742.

Guo, P., Wang, H., Qin, F., Miao, C., Zhang, F., 2023a. Coupled MOP and PLUS-SA model research on land use scenario simulations in Zhengzhou metropolitan area, Central China. Rem. Sens. 15, 3762. https://doi.org/10.3390/rs15153762.

Guo, X., Zhang, Y., Guo, D., Lu, W., Xu, H., 2023b. How does ecological protection redline policy affect regional land use and ecosystem services? Environ. Impact Assess. Rev. 100, 107062. https://doi.org/10.1016/j.eiar.2023.107062.
Hack, J., Molewijk, D., Beißler, M.R., 2020. A conceptual approach to modeling the geospatial impact of typical urban threats on the habitat quality of river corridors. Remote Sens. (Basel) 12 (8), 1345. https://doi.org/10.3390/rs12081345.
Hu, P., Zhou, Y., Zhou, J., Wang, G., Zhu, G., 2022. Uncovering the willingness to pay for ecological red lines protection: evidence from China. Ecol. Ind. 134, 108458. https://doi.org/10.1016/j.ecolind.2021.108458.
Hua, T., Zhao, W., Cherubini, F., Hu, X., Pereira, P., 2022. Strengthening protected areas for climate refugia on the Tibetan Plateau, China. Biol. Conserv. 275, 109781. https://doi.org/10.1016/j.biocon.2022.109781.
Jian, Z., Sun, Y., Wang, F., Zhou, C., Pan, F., Meng, W., et al., 2024. Soil conservation ecosystem service supply-demand and multi-scenario simulation in the Loess Plateau, China. Global Ecol. Conserv. 49, e2796.
Ke, X., Van Vliet, J., Zhou, T., Verburg, P.H., Zheng, W., Liu, X., 2018. Direct and indirect loss of natural habitat due to built-up area expansion: a model-based analysis for the city of Wuhan, China. Land Use Policy 74, 231–239. https://doi.org/10.1016/j.landusepol.2017.12.048.
Kumar, V., Kedam, N., Sharma, K.V., Mehta, D.J., Caloiero, T., 2023. Advanced machine learning techniques to improve hydrological prediction: a comparative analysis of streamflow prediction models. Water 15 (14), 2572. https://doi.org/10.3390/w15142572.
Li, M., Liu, S., Wang, F., Liu, H., Liu, Y., Wang, Q., 2022. Cost-benefit analysis of ecological restoration based on land use scenario simulation and ecosystem service on the Qinghai-Tibet Plateau. Global Ecol. Conserv. 34, e02006.
Liang, X., Guan, Q., Clarke, K.C., Liu, S., Wang, B., Yao, Y., 2021. Understanding the drivers of sustainable land expansion using a patch-generating land use simulation (PLUS) model: a case study in Wuhan, China. Comput. Environ. Urban Syst. 85, 101569. https://doi.org/10.1016/j.compenvurbsys.2020.101569.
Liang, Y., Song, W., 2022. Ecological and environmental effects of land use and cover changes on the Qinghai-Tibetan plateau: a bibliometric review. Land 11 (12), 2163. https://doi.org/10.3390/land11122163.
Lin, X.F., Fu, H., 2023. Multi-scenario simulation analysis of cultivated land based on PLUS model-a case study of Haikou, China. Front. Ecol. Evol. 11, 1197419. https://doi.org/10.3389/fevo.2023.1197419.
Liu, B., 2021. Actual livestock carrying capacity estimation product in Qinghai-Tibet Plateau (2000–2019). National Tibetan Plateau/Third Pole Environment Data Center. https://doi.org/10.11888/Ecolo.tpdc.271513.
Liu, H.M., Chen, H., 2023. Third Pole needs more than legal protection. Science 382, 1254. https://doi.org/10.1126/science.adl5035.
Liu, H., Cheng, Y., Liu, Z., Li, Q., Zhang, H., Wei, W., 2023b. Conflict or coordination? The spatiotemporal relationship between humans and nature on the Qinghai-Tibet Plateau. Earth's Future 11 (9). https://doi.org/10.1029/2022EF003452 e2022EF003452.
Liu, C., Liu, D., Li, P., Li, X., Liu, Z., Zhao, Y., 2023a. Assessment of occupation of natural habitat by urban expansion and its impact on crucial ecosystem services in China's coastal zone. Ecol. Ind. 154, 110682. https://doi.org/10.1016/j.ecolind.2023.110682.
Liu, L., Zhao, G., An, Z., My, X., Jiao, J., An, S., et al., 2022. Effect of grazing intensity on alpine meadow soil quality in the eastern Qinghai-Tibet Plateau, China. Ecol. Ind. 141, 109111. https://doi.org/10.1016/j.ecolind.2022.109111.
Moayedi, H., Canatalay, P.J., Dehrashid, A.A., Cifci, M.A., Salari, M., Le, B.N., 2023. Multilayer Perceptron and Their Comparison with Two Nature-Inspired Hybrid Techniques of Biogeography-Based Optimization (BBO) and Backtracking Search Algorithm (BSA) for Assessment of Landslide Susceptibility. Land 12 (1), 242. https://doi.org/10.3390/land12010242.
Munthali, M.G., Kindu, M., Adeola, A.M., Davis, N., Botai, J.O., Solomon, N., 2023. Variations of ecosystem service values as a response to land use and land cover dynamics in central Malawi. Environ. Develop. Sustain. 25, 9821–9837. https://doi.org/10.1007/s10668-022-02461-w.
Nie, W., Xu, B., Yang, F., Shi, Y., Liu, B., Lin, W., et al., 2023. Simulating future land use by coupling ecological security patterns and multiple scenarios. Sci. Total Environ. 859, 160262. https://doi.org/10.1016/j.scitotenv.2022.160262.
Nie, Y., Yang, Y., Wang, Y., Liu, Z., He, C., Chen, X., 2022. Comprehensive impacts of urban expansion on natural habitat quality in Chengguan District of Lhasa City in recent 50 years. Acta Ecol. Sinica 43 (6), 2202–2220. https://doi.org/10.5846/stxb202102100423. In Chinese with English abstract.
Peng, S., 2020. 1-km monthly precipitation dataset for China (1901–2022). National Tibet Plateau / Third Pole Environment Data Center. https://doi.org/10.5281/zenodo.3185722.
Peng, S., 2023. 1-km monthly mean temperature dataset for China (1901–2022). National Tibetan Plateau / Third Pole Environment Data Center. https://cstr.cn/18406.11.Meteoro.tpdc.270961.
Qiushi (2023). China passes landmark law to protect Qinghai-Tibet Plateau ecosystem http://en.qstheory.cn/2023-04/27/c_881812.htm# (accessed 23 September 2024).
Song, X., Yang, G., Yan, C., Duan, H., Liu, G., Zhu, Y., 2009. Driving forces behind land use and cover change in the Qinghai-Tibetan Plateau: a case study of the source region of the Yellow River, Qinghai Province, China. Environ. Earth Sci. 59, 793–801. https://doi.org/10.1007/s12665-009-0075-8.
Sun, N., Chen, Q., Liu, F., Zhou, Q., He, W., Guo, Y., 2023b. Land use simulation and landscape ecological risk assessment on the Qinghai-Tibet plateau. Land 12 (4), 923. https://doi.org/10.3390/land12040923.
Sun, L., Li, H., Wang, J., Chen, Y., Xiong, N., Wang, Z., et al., 2023a. Impacts of climate change and human activities on NDVI in the Qinghai-Tibet plateau. Remote Sens. (Basel) 15 (3), 587. https://doi.org/10.3390/rs15030587.
Venter, O., Sanderson, E.W., Magrach, A., Allan, J.R., Beher, J., Jones, K.R., et al., 2016. Global terrestrial Human Footprint maps for 1993 and 2009. Sci. Data 3, 160067. https://doi.org/10.1038/sdata.2016.67.
Wang, Z., Guo, M., Zhang, D., Chen, R., Xi, C., Yang, H., 2023b. Coupling the calibrated GlobalLand30 data and modified PLUS model for multi-scenario land use simulation and landscape ecological risk assessment. Remote Sens. (Basel) 15 (21), 5186. https://doi.org/10.3390/rs15215186.
Wang, Z., Fu, B., Wu, X., Wang, S., Li, Y., Feng, Y., et al., 2024. Distinguishing trajectories and drivers of vegetated ecosystems in China's Loess plateau. Earth's Future 12 (2). https://doi.org/10.1029/2023EF003769.
Wang, Y., Liu, Z., He, C., Xia, P., Liu, Z., Liu, H., 2020. Quantifying urbanization levels on the Tibetan Plateau with high-resolution nighttime light data. Geogr. Sustainability 1 (3), 233–244. https://doi.org/10.1016/j.geosus.2020.08.004.
Wang, H., Liu, X., Zhao, C., Y, C., Liu, Y., Zang, F., 2021. Spatial-temporal pattern analysis of landscape ecological risk assessment based on land use/land cover change in Baishuijiang National nature reserve in Gansu Province, China. Ecol. Ind. 124, 107454. https://doi.org/10.1016/j.ecolind.2021.107454.
Wang, X., Yang, S., Yang, R., Yang, Z., 2023a. Analysis of the spatiotemporal evolution and factors influencing ecological land in northwest Yunnan from the perspective of leading the construction of a national ecological civilization. Diversity Basel 15 (10), 1074. https://doi.org/10.3390/d15101074.
Wang, H., Zhou, X., Wan, C., Fu, H., Zhang, F., Ren, J., 2008. Eco-environmental degradation in the northeastern margin of the Qinghai-Tibetan Plateau and comprehensive ecological protection planning. Environ. Geol. 55 (5), 1135–1147.
Williams, B.A., Venter, O., Allan, J.R., Atkinson, S.C., Rehbein, J.A., Ward, W., et al., 2020. Change in terrestrial human footprint drives continued loss of intact ecosystems. One Earth 3 (3), 371–382. https://doi.org/10.1016/j.oneear.2020.08.009.
Wyatt, K.H., Griffin, R., Guerry, A.D., Ruckelshaus, M., Fogarty, M., Arkema, K.K., et al., 2017. Habitat risk assessment for regional ocean planning in the U.S. Northeast and Mid-Atlantic. PLoS One 12 (12), e0188776.
Xu, Y., Li, F., Asgari, A., 2022. Prediction and optimization of heating and cooling loads in a residential building based on multi-layer perceptron neural network and different optimization algorithms. Energy 240, 122692. https://doi.org/10.1016/j.energy.2021.122692.
Xue, J., Li, Z., Du, F., Ruan, J., Gui, J., 2023. Dynamics changes and prediction of ecosystem services in the Qinghai-Tibet Plateau, western China. Global Ecol. Conserv. 47, e2674.
Yang, Z., Ni, W., Niu, F., Li, L., Ren, S., 2024. Spatiotemporal distribution characteristics and influencing factors of freeze-thaw erosion in the Qinghai-Tibet plateau. Remote Sens. (Basel) 16 (9), 1629. https://doi.org/10.3390/rs16091629.
Yu, H., Qian, X., Jing, H., Liu, Y., 2024b. Spatiotemporal evolution characteristics and the driving force of habitat quality in the Qinghai-Tibet Plateau in topographic view (2000–2020). Front. Ecol. Evol. 12. https://doi.org/10.3389/fevo.2024.1345665.
Yu, B., Zang, Y., Wu, C., Zhao, Z., 2024a. Spatiotemporal dynamics of wetlands and their future multi-scenario simulation in the Yellow River Delta, China. J. Environ. Manage. 353 (27), 120193. https://doi.org/10.1016/j.jenvman.2024.120193.
Zeng, R., Xu, Y., Yang, L., Ai, J., Liu, C., Lu, W., 2024. Adjustment of the marine ecological red lines in China. Sci. Rep. 14, 19247. https://doi.org/10.1038/s41598-024-69606-x.
Zhang, C., Dong, Q., Chu, H., Shi, J., Li, S., Wang, Y., et al., 2018. Grassland community composition response to grazing intensity under different grazing regimes. Rangel. Ecol. Manage. 71 (2), 196–204. https://doi.org/10.1016/j.rama.2017.09.007.
Zhang, C., Wen, C.Y., Juan, Y.H., Lee, Y.T., Chen, Z., Yang, A.S., et al., 2024. Accelerating flow simulations in the built environment by using the fast fluid dynamics initializer. Build. Environ. 253 (1), 111274. https://doi.org/10.1016/j.buildenv.2024.111274.
Zhang, S., Wu, T., Guo, L., Zhao, Y., 2023. Assessing ecological risk on the Qinghai-Tibet Plateau based on future land use scenarios and ecosystem service values. Ecol. Ind. 154, 110769. https://doi.org/10.1016/j.ecolind.2023.110769.
Zhang, Y., Zhang, C., Zhang, X., Wang, X., Li, Z., Lin, Q., 2022. Habitat quality assessment and ecological risks prediction: an analysis in the Beijing-Hangzhou grand canal (Suzhou section). Water 14 (17), 2602. https://doi.org/10.3390/w14172602.
Zhao, C., Su, S., Gong, Z., Lv, C., Li, N., Luo, Q., et al., 2023. Effectiveness of protected areas in the Three-river Source Region of the Tibetan Plateau for biodiversity and ecosystem services. Ecol. Ind. 2 (154), 110861. https://doi.org/10.1016/j.ecolind.2023.110861.
Zhou, W., Wang, T., Xiao, J., Wang, K., Yu, W., Du, Z., 2024. Grassland productivity increase was dominated by climate in Qinghai-Tibet Plateau from 1982 to 2020. J. Clean. Prod. 434, 140144. https://doi.org/10.1016/j.jclepro.2023.140144.
Zhu, S., Li, L., Wu, G., Slate, T., Guo, H., Li, D., 2022. Assessing the impact of village development on the habitat quality of Yunnan snub-nosed monkeys using the INVEST model. Biology 11 (10), 1487. https://doi.org/10.3390/biology11101487.